Cell Tissue Res (2018) 372:99–114
DOI 10.1007/s00441-017-2765-y

REGULAR ARTICLE

MiR-375 inhibits the hepatocyte growth factor-elicited migration of mesenchymal stem cells by downregulating Akt signaling

Lihong He[1] · Xianyao Wang[1] · Naixin Kang[1] · Jianwei Xu[1,2] · Nan Dai[1] · Xiaojing Xu[1] · Huanxiang Zhang[1]

Received: 23 October 2016 / Accepted: 4 September 2017 / Published online: 10 January 2018

Abstract The migration of mesenchymal stem cells (MSCs) is critical for their use in cell-based therapies. Accumulating evidence suggests that microRNAs are important regulators of MSC migration. Here, we report that the expression of miR-375 was downregulated in MSCs treated with hepatocyte growth factor (HGF), which strongly stimulates the migration of these cells. Overexpression of miR-375 decreased the transfilter migration and the migration velocity of MSCs triggered by HGF. In our efforts to determine the mechanism by which miR-375 affects MSC migration, we found that miR-375 significantly inhibited the activation of Akt by downregulating its phosphorylation at T308 and S473, but had no effect on the activity of mitogen-activated protein kinases. Further, we showed that 3'phosphoinositide-dependent protein kinase-1 (PDK1), an upstream kinase necessary for full activation of Akt, was negatively regulated by miR-375 at the protein level. Moreover, miR-375 suppressed the phosphorylation of focal adhesion kinase (FAK) and paxillin, two important regulators of focal adhesion (FA) assembly and turnover, and decreased the number of FAs at cell periphery. Taken together, our results demonstrate that miR-375 inhibits HGF-elicited migration of MSCs through downregulating the expression of PDK1 and suppressing the activation of Akt, as well as influencing the tyrosine phosphorylation of FAK and paxillin and FA periphery distribution.

Keywords Mesenchymal stem cells (MSCs) · miR-375 · Hepatocyte growth factor (HGF) · Akt signaling · PDK1 · Focal adhesions (FAs) · Cell migration

Lihong He and Xianyao Wang contributed equally to this work.

✉ Huanxiang Zhang
hzhang@suda.edu.cn

Lihong He
helh@suda.edu.cn

Xianyao Wang
wangxianyao2013@163.com

Naixin Kang
carnation518@hotmail.com

Jianwei Xu
363912577@qq.com

Nan Dai
1145966995@qq.com

Xiaojing Xu
xuxiaojing@suda.edu.cn

[1] Department of Cell Biology, Jiangsu Key Laboratory of Stem Cell Research, Medical College of Soochow University, Suzhou 215123, China

[2] Tissue Engineering and Stem Cell Research Center, Guizhou Medical University, Guiyang 550004, China

Introduction

Mesenchymal stem cells (MSCs) are multipotent adult stem cells that can be easily isolated and cultured in vitro. They can be differentiated into mesodermal lineages, such as chondrocytes, osteocytes and adipocytes, and nonmesodermal lineages, for example, neuronal cells and hepatocytes (Bianco et al. 2001; Cho et al. 2005; Dezawa et al. 2004; Luk et al. 2005; Stock et al. 2010). The versatility, easy availability, low immunogenicity, immunomodulatory function and lack of ethical controversy make MSCs excellent candidates for cell replacement therapies to treat a wide variety of clinical pathologies (Abdallah and Kassem 2008; Murphy et al. 2013).

MSCs are usually administered by intravenous or artery infusion, intraperitoneal injection, or by placement of cells near the lesion site (El-Hossary et al. 2016; English et al. 2010;

Kwon et al. 2014; Marconi et al. 2012; Parr et al. 2007; Wang et al. 2016). Therefore, migration of MSCs toward the pathological sites is essential for their clinical use. Growth factors and chemokines released from tissues around pathology, such as hepatocyte growth factor (HGF) and vascular endothelial growth factor (VEGF), stimulate the migration of MSCs to the pathological sites (Forte et al. 2006; Ponte et al. 2007; Schenk et al. 2007; Sordi et al. 2005). Multiple signaling pathways, including the phosphatidylinositol 3-kinase (PI3K)/Akt, and mitogen-activated protein kinase (MAPK) signaling pathways (Ryu et al. 2010; Xu et al. 2014; Zheng et al. 2013), are involved in the regulation of MSC migration. Much is still unknown, however, about the detailed mechanisms that regulate the migration of MSCs upstream or downstream of the PI3K/Akt and MAPK signaling pathways.

Recent studies have demonstrated that microRNAs (miRNAs) can act upstream of signaling pathways to regulate cell migration, invasion or metastasis (Huang and He 2010). MiRNAs, the evolutionarily conserved noncoding small RNA molecules typically of 19–23 nucleotides, are considered as master regulators of almost all aspects of cell biology because miRNAs can simultaneously regulate the expression of hundreds or even thousands of mRNA targets (Im and Kenny 2012). They usually act through binding to the 3'untranslated region (3'UTR) of target mRNAs by incomplete complementation with their 5'end seed region, leading to translational suppression or degradation of target mRNAs (Im and Kenny 2012). Recently, miR-1, miR-206 and miR-34a have been reported to inhibit rhabdomyosarcoma and hepatocellular carcinoma cell (HCC) migration by targeting the HGF receptor c-Met and decreasing the phosphorylation of extracellular signal-related protein kinase 1/2 (ERK1/2) (Li et al. 2009; Yan et al. 2009); miR-21, miR-221 and miR-222 promote HCC migration and invasion by targeting phosphatase and tensin homolog deleted on chromosome ten (PTEN) and increasing Akt activity (Garofalo et al. 2009; Meng et al. 2007). MiR-335 and miR-10b have been reported to affect MSC migration by targeting RUNX2 and E-cadherin, respectively (Tome et al. 2011; Zhang et al. 2013). However, it is largely unknown how miRNAs regulate the migration of MSCs or about their interactions with PI3K/Akt and MAPK signaling pathways in regulating MSC migration. To gain further insight into this, we performed microarray assays to find miRNAs that differentially expressed in MSCs upon stimulation with HGF, the well-known chemoattractant that strongly induces MSC migration (Forte et al. 2006; Zheng et al. 2013). We hypothesized that miRNAs that are significantly downregulated or upregulated by HGF may be essential regulators of MSC locomotive response. In this study, we report that miR-375, one HGF-downregulated miRNA, inhibits the migration of MSCs elicited by HGF through suppressing Akt signaling. Decreased FAK and paxillin phosphorylation and FA periphery distribution might also contribute to the inhibition of MSC migration by miR-375.

Materials and methods

Culture and characterization of MSCs

The isolation, cultivation and characterization of MSCs were performed as previously described (Zheng et al. 2013). In brief, primary rat bone marrow-derived MSCs were isolated from the total bone marrow of femurs and tibias of 4- to 5-week-old male Sprague-Dawley rats (100–150 g) and cultured in the standard medium composed of low-glucose Dulbecco's modified Eagle's medium (L-DMEM; Gibco), supplemented with 10% fetal bovine serum (FBS; Gibco), 2 mM L-glutamine, 100 units/ml penicillin, and 100 μg/ml streptomycin. Cells were incubated in 5% CO_2 at 37 °C and the media were replaced first at 24 h, then every 3 days. Non-adherent cells were removed by changing the culture media. MSCs at 80–90% confluence were dissociated with 0.25% trypsin-EDTA solution (Sigma) and subcultured at a ratio of 1:2. All animal experiments were conducted in accordance with the guidelines for animal use approved by Soochow University Veterinary Authority. Immunophenotypic characterization of MSCs was evaluated through direct or indirect immunofluorescence with CD34-fluorescein isothiocyanate (FITC), CD45-FITC, CD29-FITC, CD90-FITC, and CD106-PE (1:200; Cedarlane). MSCs at 80–90% confluence were submitted for differentiation evaluation. Osteogenic differentiation was tested by the calcium cobalt method to identify the alkaline phosphatase after maintenance for 30 days with induction medium [L-DMEM supplemented with 10% newborn calf serum (NC; Gibco), 100 nM dexamethasone, 10 mM sodium β-glycerophosphate, and 0.05 mM L-ascorbic acid 2-phosphate (Sigma)], which was replaced every 3–4 days. Adipogenic differentiation was tested for lipid accumulation by oil red O staining after incubation for 6 days with induction medium [high-glucose Dulbecco's modified Eagle's medium (H-DMEM; Gibco), supplemented with 10% NCS, 1 mM dexamethasone, 10 mg/ml insulin, 0.2 mM indomethacin, and 0.5 mM 3-isobutyl-1-methyl-xanthine (Sigma)] and then 9 days with maintenance medium (H-DMEM, 0.01 mg/ml insulin, and 10% NCS). MSCs at passages 4–10 were used for experiments. At approximately 60–70% confluence, cells were infected with recombinant adenovirus to overexpress miR-375.

Generation of recombinant adenoviral vector

Overexpression of miR-375 was achieved by infecting MSCs with Ad-375, a recombinant adenovirus containing the miR-375 precursor sequence, or with Ad, an adenovirus with no inserted miRNA precursor sequence. as control. To generate the recombinant adenoviral vectors expressing miR-375 (Ad-375), a fragment containing the miR-375 hairpin sequence flanked by 250 bp upstream and 250 bp downstream of the

genomic sequence was amplified by PCR from rat genomic DNA with primers containing BglIIand XhoI: 5′-TACA GATCTCGGCAGCTCAGAGTCTG -3′ and 5′-AACT CGAGGCAGAAACTCCGTGGCG-3′. The fragment was inserted into the shuttle vector pAdTrack-CMV (Stratagene), then transferred to the AdEasy-1 plasmid through homologous recombination, and finally packaged in QBI-HEK293A cells (Stratagene) to generate viruses. The control virus (Ad) was derived from the same vector system. Both Ad and Ad-375 carry the green fluorescent protein (GFP), which can be observed in MSCs after 24–36 h infection. The viruses were titered, and MSCs were infected at a multiplicity of infection (MOI) of 150.

Analysis of miRNA and mRNA expression

Expression of miR-375 and its target 3'phosphoinositide-dependent protein kinase-1 (PDK1) transcript was analyzed by quantitative PCR (qPCR). Total RNA was extracted with TRIzol (Invitrogen) and treated with RQ1 RNase-free DNase (Promega). cDNA was generated with RevertAid First Strand cDNA Synthesis Kits (Thermo Scientific) using specific stem-loop RT primers for miRNAs (RiboBio) and Oligo$(dT)_{18}$ primer (Thermo Scientific) for mRNAs. Real-time PCR was by a Bio-Rad CFX96 system using SsoFast EvaGrean Supermix (Bio-Rad). Specific Bulge-Loop forward and reverse primers (RiboBio) were used to amplify miR-375 and snU6. Specific primers for *PDK1* were 5′-AAGG GTACGGGCCTCTCAAA-3′ (forward) and 5′-GGGA GTGGGAAGAGGAGGAT-3′ (reverse), and for *GAPDH* were 5′-TGACAACTTTGGCATCGTGG-3′ (forward) and 5′-TACTTGGCAGGTTTCTCCAGG-3′ (reverse). Data were calculated with Bio-Rad CFX manager software v.2.1 by the $\Delta\Delta C_T$ method (Livak and Schmittgen 2001) and expressed as relative quantities after snU6 or *GAPDH* normalization.

Western blot analysis

Western blot analysis was performed as previously described (Zheng et al. 2013). Briefly, after serum-starvation for 30 min, MSCs were treated with 50 ng/ml HGF (PeproTech) or L-DMEM for the indicated time, then exposed to liquid nitrogen and lysed with a protein extraction reagent (25 mM Tris-HCl, pH 7.2, 150 mM NaCl, 1% Triton X-100, 1% sodium deoxycholate, 1 mM EDTA, 0.1% sodium dodecyl sulfate (SDS), 1% phenylmethylsulfonyl fluoride, and 1 mM $NaVO_3$). Lysates were centrifuged at 12,000 rpm and 4 °C for 10 min to remove cell debris. The supernatants were transferred to fresh tubes, and protein concentrations were determined by BCA assay kit (Applygen). Identical amounts of protein lysates were separated using 10% SDS-PAGE gels and transferred to a 0.45-mm nitrocellulose membrane (Millipore) at a constant 2.5 mA/cm^2 for 30 min using a Trans-Blot SD Semi-Dry electrophoretic Transfer Cell (Bio-Rad). After blocking with 5% nonfat milk in TBST (100 mM Tris-HCl, pH 7.4, 150 mM NaCl, with 0.1% Tween-20), the membrane was precipitated with primary Abs for phospho- or nonphospho-protein kinases overnight at 4 °C. Membranes were then washed three times (10 min each) with TBST, and incubated with the appropriate horseradish peroxidase-linked secondary antibodies for 1 h at room temperature. Beta-actin on the same membrane served as the loading control. Primary antibodies (Abs) for phospho- or nonphospho-kinases [rabbit mAb antiphospho-ERK1/2 (Thr202/Tyr204), rabbit mAb anti-ERK1/2, rabbit mAb antiphospho-Akt (Thr308, Ser473), rabbit mAb anti-Akt, rabbit mAb antiphospho-SAPK/JNK (Thr183/Tyr185), rabbit mAb anti-SAPK/JNK, rabbit mAb antiphospho-p38MAPK (Thr180/Tyr182), rabbit mAb anti-p38MAPK, rabbit mAb antiphospho-FAK (Tyr397), rabbit mAb anti-FAK; Cell Signaling Technologies; rabbit Ab antiphospho-paxillin (Tyr118) and rabbit Ab anti-paxillin; Santa Cruz Biotechnology] were used at 1:1000 dilution. Appropriate horseradish peroxidase-linked secondary antibodies (Cell Signaling Technologies) were used at 1:2000 dilution. Antigen-antibody complexes were visualized by enhanced chemiluminescence (Biological Industries). Proteins of quite distinct molecular weight, p38MAPK together with ERK1/2 and SAPK/JNK, Akt together with paxillin, and FAK, were separately probed by cutting the nitrocellulose membrane according to the protein molecular weight marker. After detection of phospho-proteins, the membranes were incubated in Stripping Solution (Applygen Technologies) for 30 min at room temperature to strip off the first set of protein probes. After washing three times (10 min each) with TBST, the stripped blots were blocked and re-probed with the second set of primary and secondary antibodies for detection of nonphospho-proteins. Densitometry analysis was performed by gel image analysis software (ImageJ; NIH) and the relative intensity of phospho- to total protein was calculated. Data shown are the averages of three different experiments.

Boyden chamber migration assay

Transfilter migration of MSCs toward HGF was studied using a 48-well modified Boyden chamber (Neuro Probe). After 48 h infection of Ad-375 or Ad, MSCs were starved with serum-free medium for 30 min, then digested with 0.25% trypsin-EDTA and resuspended with L-DMEM and adjusted to 8×10^5 cells/ml. A single-cell suspension of 50 μl was seeded into the upper chamber of each well on a poly-L-lysine (Sigma)-precoated polyvinylpyrrolidone-free polycarbonate membranes (8 μm pore size; Osmonics), and 30 μl medium with or without 50 ng/ml HGF (PeproTech) was placed in the lower chamber. Cells were incubated at 37 °C in a 5% CO_2 humidified incubator for 5 h. After incubation, the chamber was disassembled, the upper side of the filter was

wiped off, and cells attached to the lower side were fixed with 4% paraformaldehyde in 0.1 M phosphate-buffered saline (PBS), pH 7.2, then stained for 30 min in 0.1% cresyl violet and counted at ×200 magnification in all fields of each well (each condition was run in six wells in each assay).

Migration velocity and efficiency of forward migration

The individual cell migration behavior, including migration velocity and migration efficiency, was studied by direct recording of the migration trace with a Dunn chamber under a Leica DMI 6000 B microscope equipped with a CO_2 supply, temperature thermostat and a time-lapse video system, as previously described (Zheng et al. 2013). The Dunn chamber is made from a Helber bacteria counting chamber by grinding a circular well in the central platform to leave a 1-mm-wide annular bridge between the inner and the outer wells. It has been established that chemoattractants added to the outer well of the device will diffuse across the bridge to the inner well of the chamber and form a linear steady gradient. This apparatus allows for the direct monitoring of cell locomotion and the analysis of migration speed, turning behavior, and persistency of migration. The outer well of the Dunn chamber was filled with L-DMEM containing 50 ng/ml HGF and the concentric inner well of the Dunn chamber contained only L-DMEM. MSCs cultured on coverslips and infected with Ad-375 or Ad for 48 h were inverted onto a Dunn chamber, and recorded every 5 min using a ×10 objective of a Leica DMI 6000 B microscope for a period of 4 h at 37 °C. Migration traces of at least 50 sparsely distributed cells were manually tracked using ImageJ software. Migration velocity for each time-lapse interval (5 min) was calculated, and the mean velocity was derived for the recorded 4-h period. Forward migration index (FMI), an indicator of the efficiency of forward migration or migration persistency, was calculated as the ratio of forward progress (net distance progressed in the direction of HGF concentration) to total path length (total distance the cell traveled through the field).

BrdU staining

The effect of miR-375 on the proliferation of MSCs in the presence of HGF was tested by a BrdU (5-bromo-2-deoxyuridine) incorporation assay. After infection with Ad-375 or Ad for 48 h, MSCs were incorporated with 3 μg/ml BrdU (Sigma) for 24 h and treated with 50 ng/ml HGF for 5 h. Then, cells were fixed in cold 4% paraformaldehyde and stained with BrdU Flow Kits (BD Biosciences) according to the manufacturer's instructions. The proportion of BrdU-positive cells among GFP-expressing cells was quantified. More than 500 cells were counted per experiment and experiments were performed in triplicate.

Flow cytometry detection of cell apoptosis and death

Cell apoptosis and death were detected by double staining of Alexa Flour 647-conjugated Annexin-V and propidium iodide (PI; Biouniquer, BU-AP0103). MSCs infected with Ad or Ad-375 for 48 h were trypsinized, centrifuged at 1000*g* for 5 min, washed twice with cold PBS, and processed according to the manufacturer's instructions. Ten thousand cells per sample were acquired with a FACS flow cytometer (FACScan). Cell fluorescence was analyzed with flow cytometry using the Cell Quest Pro software (Beckman Coulter). Each experiment was performed in triplicates and repeated independently three times.

Immunocytochemistry and FA analysis

After 48 h infection of Ad-375 or Ad, MSCs were serum-starved for 30 min and stimulated with 50 ng/ml HGF for 0, 5, 15, 30, or 60 min. Cells were fixed in cold 4% paraformaldehyde in 0.1 M PBS (pH 7.2) overnight, washed three times with PBS (5 min) and incubated with primary rabbit polyclonal Ab against paxillin (Santa Cruz Biotechnology) diluted in PBS/0.02% NaN_3/3% bovine serum albumin (BSA)/0.2% Triton X-100 at 1:50. After incubation with primary Abs overnight at 4 °C, cells were washed with PBS three times for 10 min each before secondary antibody application. Cy3-conjugated goat anti-rabbit Ab (Proteintech) was diluted in PBS/0.02% NaN_3/3% BSA/0.2% Triton X-100 at 1:200 and applied to cells for 1 h at room temperature in the dark. Fluorescence was examined with a Leica DMI 6000 B microscope. Controls treated with nonspecific mouse IgM or secondary Abs alone showed no staining.

The numbers of FAs at the cell periphery and center were counted and FA length was measured using NIH ImageJ software from at least 15 cells as previously described (Wang et al. 2015). The number of FAs at the periphery and center were counted and the ratio of FAs at the periphery to the total was calculated to assess the effect of miR-375 on FA distribution in response to HGF treatment. The ratios of FAs of <1 μm, 1–2 μm, 2–3 μm and >3 μm to total FAs were calculated to evaluate the effect of miR-375 on FA length in response to HGF stimulation.

Statistical analysis

Data are presented as the mean ± standard error of the mean (SEM). Statistical analysis was performed with Student's *t* test or the one-way analysis of variance (ANOVA) followed by Bonferroni–Dunn or Tamhane's T2 multiple comparisons test using SPSS software. Student's *t* test was used for comparison between control and miR-375-overexpressing cells and ANOVA was used for comparison among control and miR-375-overexpressing cells treated with or without HGF for

different time intervals. Differences were considered statistically significant when $P < 0.05$.

Results

The isolation, cultivation and characterization of rat bone marrow-derived MSCs were performed as previously described (Zheng et al. 2013). The MSCs we obtained were typically fibroblast-like or long spindle-shaped and readily expressed CD29, CD90, and CD106 but not CD34 and CD45. Upon appropriate osteogenic and adipogenic induction, MSCs could differentiate into osteoblasts and adipocytes in vitro, which is consistent with previous reports (Chamberlain et al. 2007; Pittenger et al. 1999).

MiR-375 is significantly downregulated in MSCs stimulated with HGF

Emerging evidence indicates that miRNAs play an important role in cell migration by directly regulating extracellular matrix (ECM) remodeling, cell adhesion, and intracellular signalings (Huang and He 2010). To investigate the role of miRNAs in MSC migration, we have previously performed microarray analysis to identify miRNAs that differentially expressed upon HGF treatment, and found 26 miRNAs differentially expressed (Zhu et al. 2016). Among these miRNAs, miR-375 was specifically selected for functional study in light of its known inhibitory roles in chondrogenic progenitor cell migration (Song et al. 2013) and a variety of cancer cell metastasis (Kinoshita et al. 2012; Kong et al. 2012). Using stem-loop RT-qPCR we confirmed the downregulated expression of miR-375 in MSCs treated with 50 ng/ml HGF for 30 min to 12 h ($P < 0.05$; Fig. 1). The results suggest that miR-375 might be involved in regulating the migration of MSCs in response to HGF.

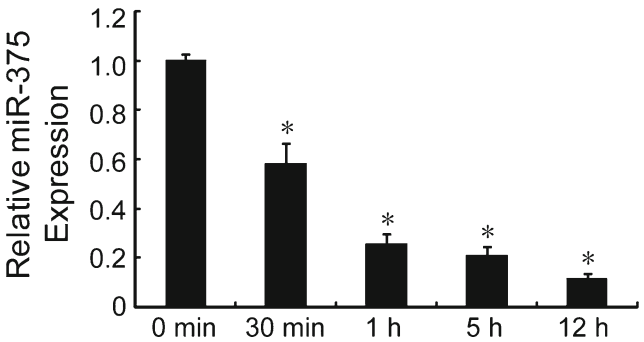

Fig. 1 HGF stimulation decreases the expression of miR-375 in MSCs. MSCs were treated with 50 ng/ml HGF for the indicated times. Stem-loop RT-qPCR was performed to quantify the expression of miR-375. Values are normalized with U6 snRNA and expressed as a percentage of control value, that is, the normalized expression value of MSCs in serum-free medium without HGF. Data represent the mean ± SEM from four independent experiments. *$P < 0.05$, compared with the control value

MiR-375 inhibits HGF-elicited migration of MSCs

To assess the influence of miR-375 on cell migration, we tested the transfilter migration of MSCs toward HGF using a Boyden chamber. Compared with control cells that exhibit chemotactic migration toward HGF, overexpression of miR-375 in MSCs by infection of adenovirus containing miR-375 precursor sequence (Ad-375), which resulted in a significantly higher expression (Fig. 2a), led to a significantly decreased number of cells that migrated toward HGF (Fig. 2b, b'). No effects of miR-375 on MSC proliferation and apoptosis were observed by BrdU incorporation (Fig. 2c, c') and flow cytometry detection (Fig. 2d, d'), respectively. These results demonstrate that miR-375 inhibits the transfilter migration of MSCs toward HGF.

MiR-375 influences migration velocity of MSCs in response to HGF

Studies from the Boyden chamber prove that overexpression of miR-375 inhibits the transfilter migration of MSCs toward HGF. However, using a Boyden chamber, it is impossible to visualize the migratory behavior in response to HGF and detail the migratory responses. To directly observe the migratory behavior of MSCs, we used time-lapse video microscopy coupled with the direct-viewing Dunn chamber, which allows one to track the movement of cells and characterize cell migration in response to HGF by migration velocity and the forward migration index (Fig. 3a–b'). We first investigated the effect of miR-375 on cell random migration, where both the outer well and the inner well of the Dunn chamber contain only L-DMEM. Results showed that neither the migration velocity nor FMI was affected by miR-375 (Fig. 3c, c'), implying that miR-375 are not involved in the random migration of MSCs.

We next analyzed the effect of miR-375 on migration behavior of MSCs in response to HGF by filling the outer well of the Dunn chamber with L-DMEM containing 50 ng/ml HGF and the inner well with L-DMEM only. MSCs grown on coverslips were inverted on the chamber and cell migration was recorded for 4 h. Results showed that migration velocity of miR-375-overexpressing MSCs was significantly lower than that of control cells (Fig. 3d), whereas no difference of FMI was detected (Fig. 3d'), suggesting that miR-375 inhibits the motility, but not the efficiency of cell migration in response to HGF.

MiR-375 influences phosphorylation of Akt in MSCs

We previously demonstrated that PI3K/Akt and MAPK signaling pathways mediate the HGF-induced migration of MSCs (Zheng et al. 2013). To explore the molecular mechanism underlying the inhibition of HGF-elicited migration of

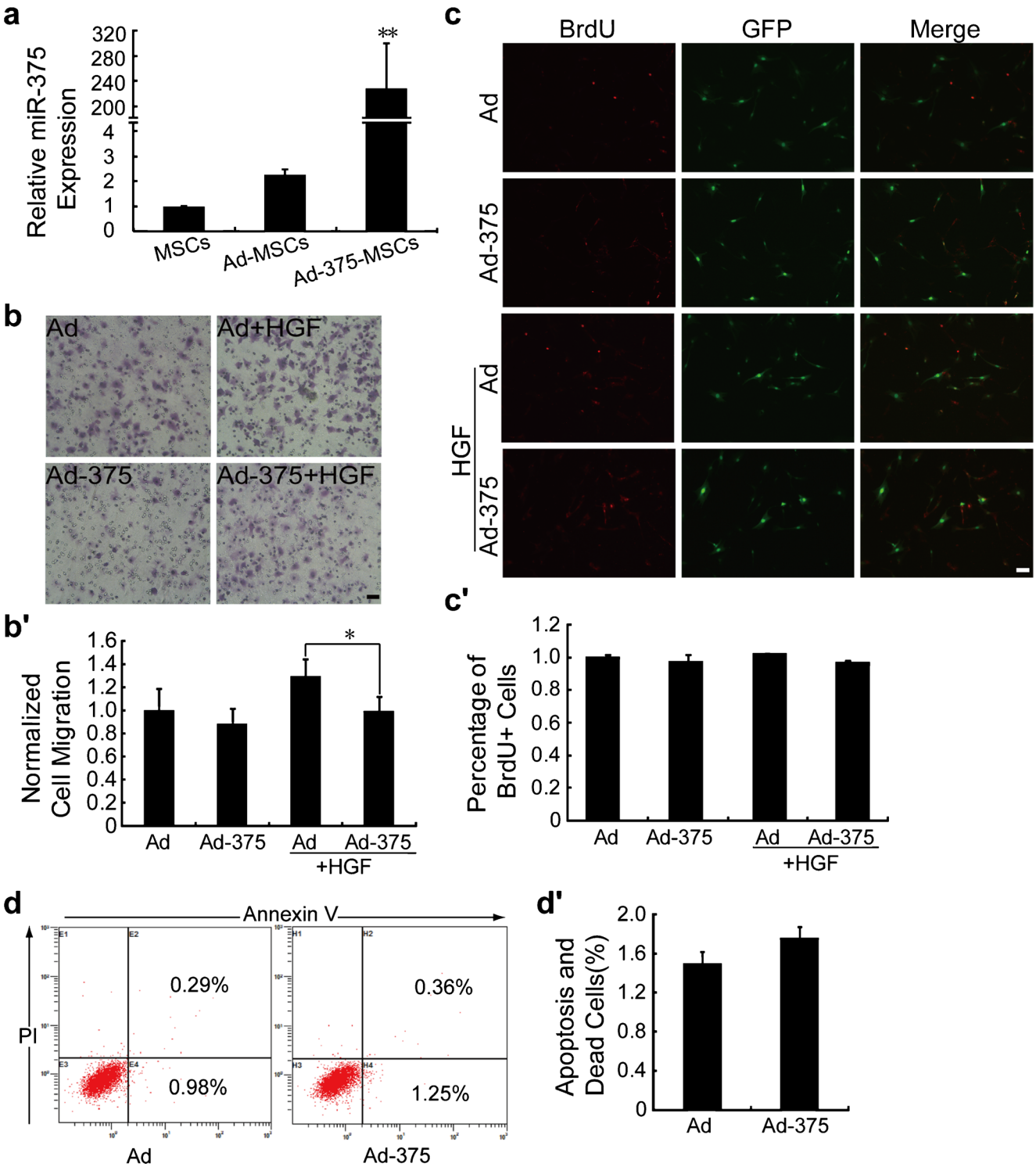

Fig. 2 Overexpression of miR-375 inhibits the transfilter migration of MSCs toward HGF. **a** Expression of miR-375 in MSCs infected with Ad or Ad-375 for 48 h by stem-loop RT-qPCR. Values are normalized with U6 snRNA and expressed as a percentage of the value in MSCs without adenovirus infection. **b**, **b'** Transfilter migration of MSCs infected with Ad or Ad-375. Images are representative of migratory cells/field on the membrane underside, *scale bar* 100 μm (**b**). Values are normalized with Ad-infected MSCs without HGF. Data represent the mean ± SEM from four independent experiments. *$P < 0.05$ (**b'**). **c**, **c'** MiR-375 does not affect the proliferation of MSCs despite the presence or absence of HGF. Shown are representative images of BrdU-positive (*red*) MSCs (**c**, *scale bar* 100 μm) and the average number of BrdU-positive cells from three independent experiments (**c'**). **d**, **d'** MiR-375 has no effect on the apoptosis of MSCs. MSCs infected with Ad or Ad-375 for 48 h were processed for flow cytometry analysis of apoptotic and dead cells after staining with Annexin V-Alexa Flour 647/PI according to the manufacturer's instruction. Cells in late stages of apoptosis were Annexin V/PI-positive (**d**). The percentage of apoptotic and dead cells in control and miR-375 overexpressing MSCs were calculated. Data shown are mean ± SEM from three independent experiments (**d'**)

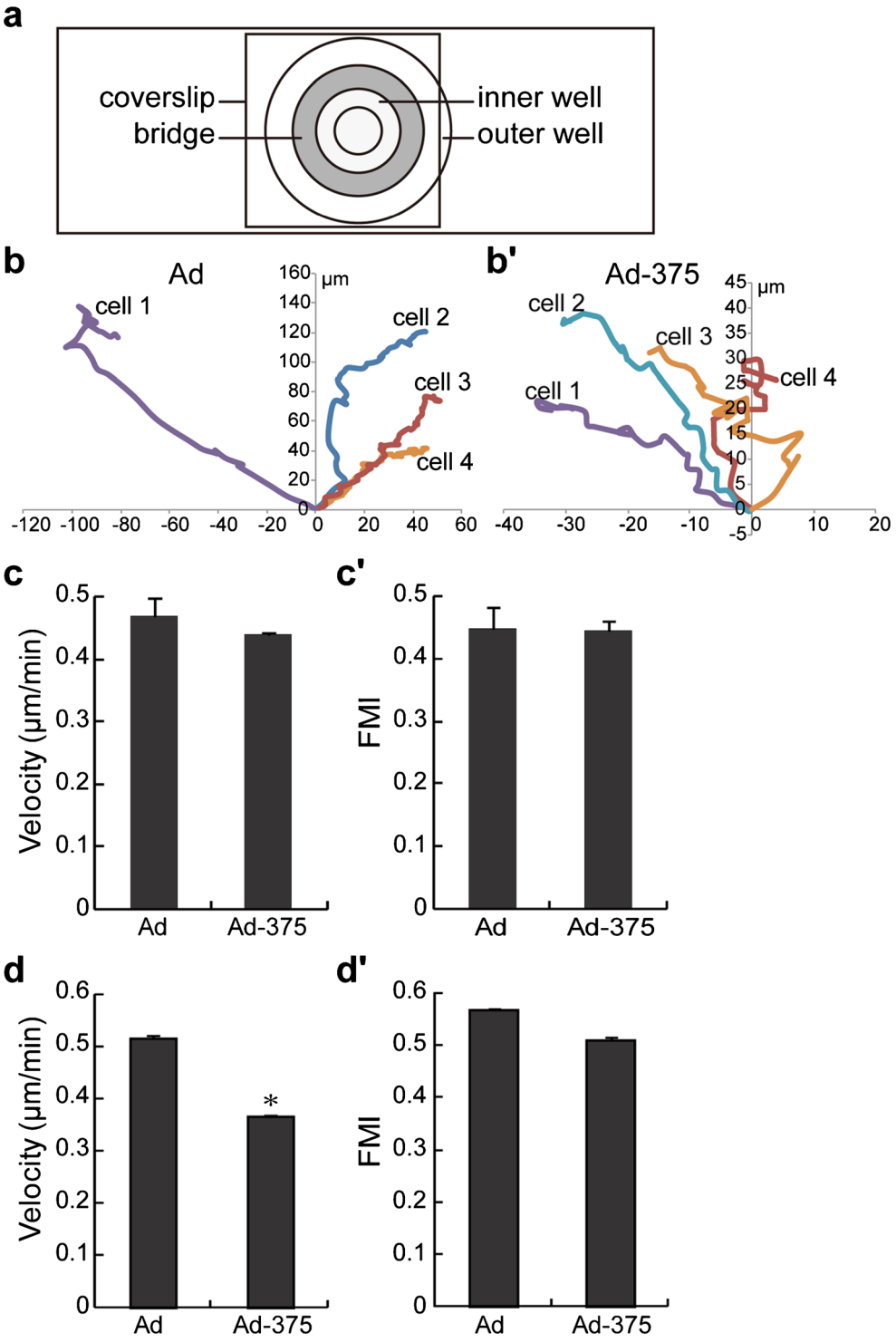

Fig. 3 Effects of miR-375 on the migration velocity (μm/min) and the forward migration index (FMI) of MSCs. **a** Schematic representation of the Dunn chamber with the overlying coverslip, showing the position of the inner well, bridge, and outer well. **b**, **b'** Migration tracks of four representative cells of Ad- or Ad-375-infected MSCs in the presence of HGF on the bridge of Dunn chamber, the starting point for each cell is the intersection between the *X*- and *Y*-axes (0, 0), and the source of HGF (50 ng/ml) is at the top of the *Y*-axes. **c**, **c'** The migration velocity and FMI of MSCs without HGF stimulation. **d**, **d'** The migration velocity and FMI of MSCs in response to HGF stimulation. Coverslips with cells infected with Ad or Ad-375 for 48 h were incubated with L-DMEM for 30 min, and then inverted on to the Dunn chamber and the cells were observed for a period of 4 h. Migration velocity was calculated for each time-lapse interval (5 min), and the mean velocity was derived for a period of 4 h. FMI was calculated as the ratio of the most direct distance the cell progressed to the total path length. Data shown are mean ± SEM from four independent experiments, and each experiment at least 50 cells from varied conditions were analyzed. $^{*}P < 0.05$ compared with control cells that infected with Ad

MSCs by miR-375, we investigated its effect on the phosphorylation of Akt and three major groups of MAPKs: ERK1/2, SAPK/JNK, and p38MAPK.

As shown in Fig. 4, overexpression of miR-375 significantly lowered the phosphorylation of Akt at Ser473 (S473-P) and Thr308 (T308-P), but showed no effect on the phosphorylation of ERK1/2, p38MAPK and SAPK/JNK (Fig. 4a, a'). Upon HGF treatment for 30 min, Akt phosphorylation at S473 but not T308 was partially rescued in miR-375-overexpressing cells, whereas the phosphorylation of ERK1/2, p38MAPK and SAPK/JNK remained unchanged (Fig. 4b, b').

Considering that the activation of Akt and MAPKs in MSCs varies over time upon HGF treatment (Zheng et al.

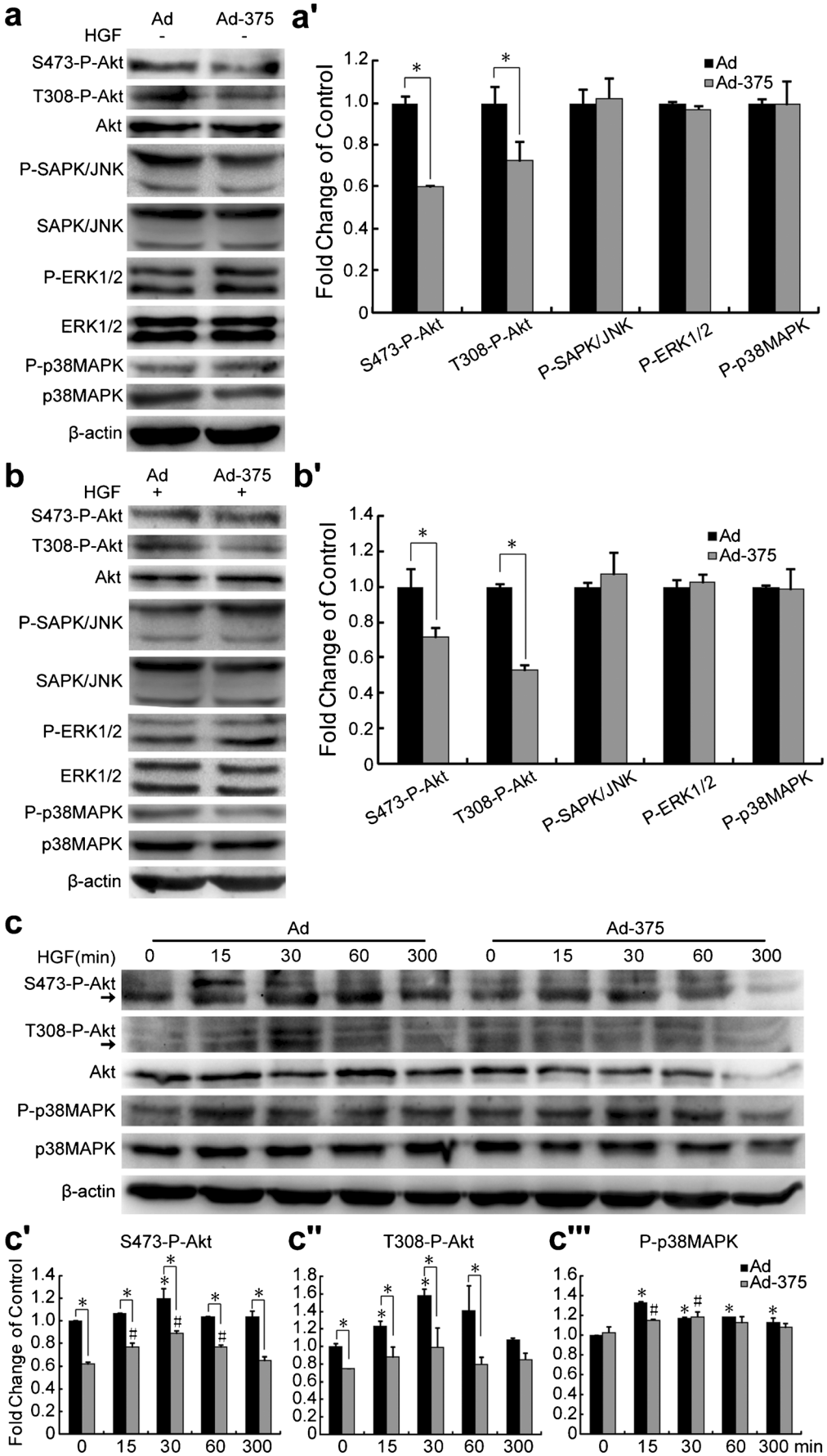
a
Ad
Ad-375
HGF
-
-
S473-P-Akt
T308-P-Akt
Akt
P-SAPK/JNK
SAPK/JNK
P-ERK1/2
ERK1/2
P-p38MAPK
p38MAPK
β-actin
a'
Fold Change of Control
Ad
Ad-375
S473-P-Akt
T308-P-Akt
P-SAPK/JNK
P-ERK1/2
P-p38MAPK
b
HGF
+
+
b'
c
HGF(min)
0
15
30
60
300
c'
S473-P-Akt
c''
T308-P-Akt
c'''
P-p38MAPK
min

◀ **Fig. 4** MiR-375 inhibits the activation of Akt but not MAPKs. **a**, **a'** The phosphorylation of Akt and MAPKs in MSCs infected with Ad-375 or Ad before HGF treatment. **b**, **b'** The phosphorylation of Akt and MAPKs in MSCs infected with Ad-375 or Ad after HGF stimulation for 30 min. **c**, **c'**, **c''**, **c'''** The phosphorylation of Akt and p38MAPK in MSCs infected with Ad-375 or Ad upon HGF treatment for indicated times. Cells were infected with Ad-375 or Ad for 48 h, and serum-starved for 30 min before stimulation with 50 ng/ml HGF or with medium only for the indicated times. Total protein extracts were analyzed by western blot using antibodies against the active phosphorylated forms or the total proteins. Equal loading of proteins were checked by β-actin. Relative level of phospho- to total protein was calculated by densitometry of immunoreactive bands using ImageJ software. Shown are representative results of three independent experiments, and data presented are mean ± SEM. *$P < 0.05$ vs. Ad without HGF, #$P < 0.05$ vs. Ad-375 without HGF

2013), to further elucidate the effect of miR-375 on Akt and MAPKs signaling pathways, MSCs were exposed to 50 ng/ml HGF for different times and the relative phosphorylation levels of Akt, ERK1/2, p38MAPK and SAPK/JNK were analyzed. As shown in Fig. 4c, c', upon exposure to HGF, Akt phosphorylation at S473 increased, peaking from 30 min to about 1 h in control cells and from 15 to about 30 min in miR-375-overexpressing cells, then decreased to basal levels at 5 h in both groups. Yet, the overall level of S473-P in miR-375-overexpressing cells remained lower than that in control cells ($P < 0.05$). Phosphorylation of Akt at T308 also increased with HGF treatment from 15 min to 1 h in control cells, while in miR-375-overexpressing cells, T308-P remained at much lower levels with no significant variation upon HGF treatment (Fig. 4c, c''). The phosphorylation levels of p38MAPK in response to HGF stimulation were comparable in control and in miR-375-overexpressing cells (Fig. 4c, c'''), and similar results were obtained in ERK1/2 and SAPK/JNK (data not shown).

Taken together, we conclude that the phosphorylation of Akt, but not MAPKs, is regulated by miR-375, suggesting that Akt signaling pathway is involved in the impact of miR-375 on HGF-elicited migration.

MiR-375 downregulates PDK1 expression in MSCs

PDK1 phosphorylates Akt at T308 and allows for its full activation (Alessi et al. 1997). Decreased phosphorylation of Akt in miR-375-overexpressing MSCs led us to investigate whether PDK1 is involved in this process. Using the miRNA target prediction tool TargetScan, we found that PDK1 is a putative target of miR-375 (Fig. 5a). Moreover, PDK1 has been demonstrated by El Ouaamari et al. (2008) as a direct target of miR-375 in rat pancreatic β-cells using the dual-luciferase reporter assay system. Consistently, in this study, we found that overexpression of miR-375 in MSCs downregulated the expression of PDK1 for about 20% at mRNA level (Fig. 5b) and for about 60% at protein level (Fig. 5c, c').

Consistent with our observation that HGF significantly downregulates the expression of endogenous miR-375 in MSCs (Fig. 1), as much as a 2.6-fold decrease of miR-375 expression was observed in Ad-375-infected MSCs up to 12 h upon HGF treatment (Fig. 5e), which, in turn, might rescue the expression of PDK1 decreased by exogenous miR-375. Indeed, western blot analysis revealed an elevated protein level of PDK1 in MSCs overexpressing miR-375 after HGF treatment for 30 min to 1 h (Fig. 5d, d'), and this partial elevation of PDK1 might contribute to the slight increase of Akt phosphorylation at T308 in these cells (Fig. 4c, c'').

MiR-375 affects the length and distribution of focal adhesions in MSCs

During migration, a cell continuously forms focal adhesions (FAs) to grasp the substrate at the cell front to generate traction forces for movement, and detaches from the substrate by disassembly of FAs at the rear part so as to move the body forward. Akt has been proved to promote fibroblast migration through promoting the disassembly of FAs (Higuchi et al. 2013). We thus investigated whether miR-375 affects the formation and distribution of FAs in MSCs.

After stimulation with HGF for different times, cells were immunostained with antibodies against paxillin to indicate FAs (Fig. 6a). The length of FAs was measured and the number of FAs at the cell periphery and center were counted. We divided the FAs into four groups according to the length: <1 μm, 1–2 μm, 2–3 μm, and >3 μm,as FAs of different length exhibit different dynamic behavior of disassembly and maturation (Parsons et al. 2010). The number of FAs belonging to a length group versus total number of FAs was calculated to describe the ratio of FAs of different length. FAs <1.0 μm were the predominant whether or not miR-375 was overexpressed (Fig. 6b, b'). Upon HGF treatment, the ratio of FAs of length 1–2 μm significantly increased in control cells ($P < 0.05$; Fig. 6b); by contrast, in MSCs overexpressing miR-375 HGF treatment just increased the ratio of FAs that were less than 1 μm at 15 min (Fig. 6b'). These results suggest that miR-375 influences the length of FAs in response to HGF.

The ratio of FAs at the cell periphery to total number of FAs was calculated to describe the FA distribution. HGF treatment for 5–15 min significantly increased the ratio of FAs at the periphery in both control and miR-375-overexpressing cells. However, the overall ratio of peripheral FAs in miR-375-overexpressing cells remained lower than control cells at all HGF treatment times except 5 min ($P < 0.05$; Fig. 6c). These results indicate that miR-375 inhibits the peripheral distribution of FAs.

MiR-375 influences the phosphorylation of FAK and paxillin in MSCs

Adhesion organization and dynamics are regulated by tyrosine phosphorylation of FA proteins, focal adhesion kinase (FAK)

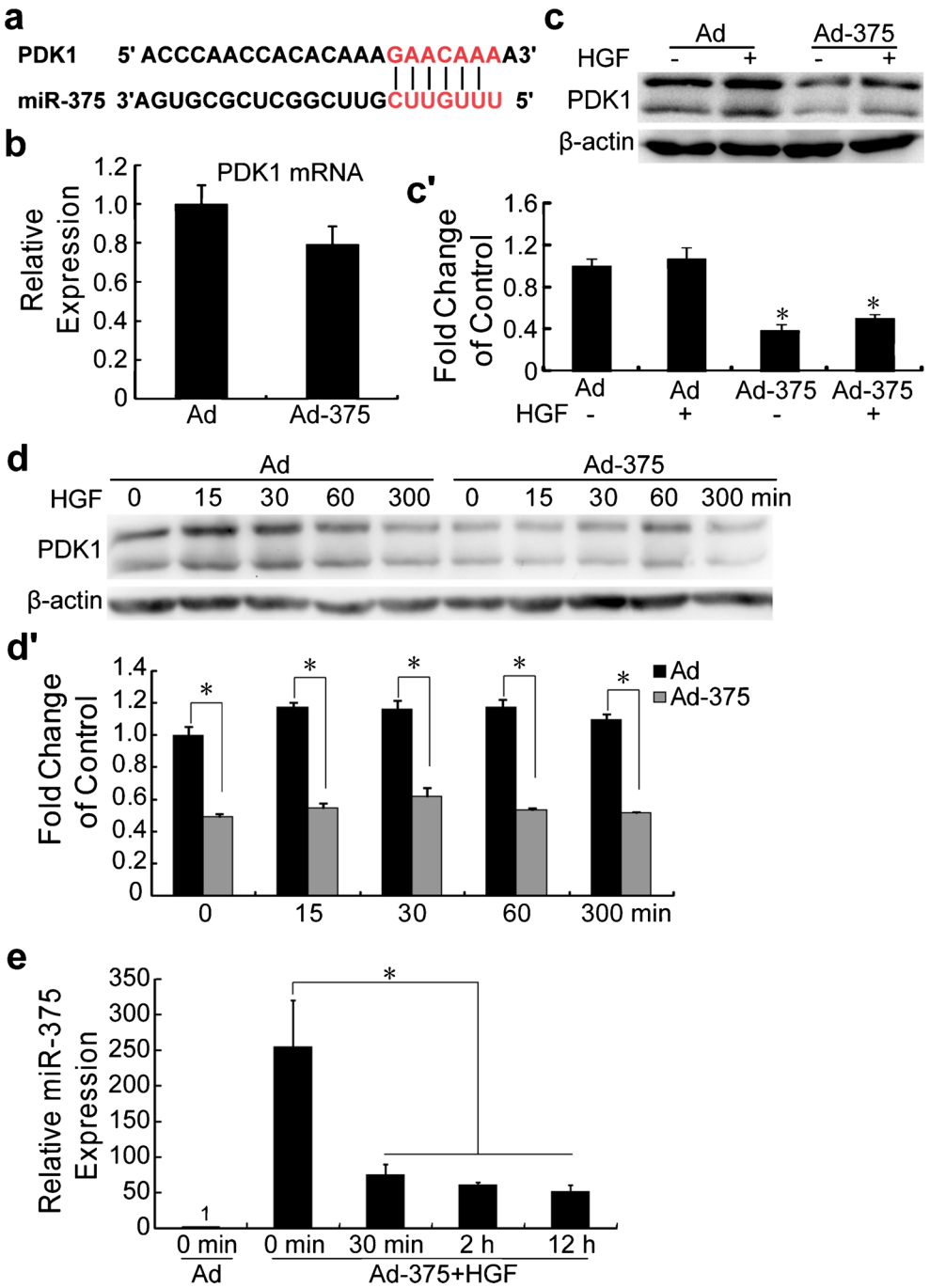

Fig. 5 MiR-375 downregulates the expression of PDK1 in MSCs. **a** Schematic illustration of the miR-375-binding sites in the 3'UTR of PDK1 mRNA. **b** PDK1 mRNA expression in MSCs infected with Ad-375 or Ad by RT-qPCR analysis. Expression was normalized with GAPDH mRNA levels and expressed as a percentage of Ad-infected cells. Data presented are mean ± SEM from three independent experiments. **c**, **c'** Western blot analysis of the protein levels of PDK1 in MSCs infected with Ad-375 or Ad. Cells were incubated with L-DMEM or L-DMEM containing 50 ng/ml HGF for 30 min after starvation for 30 min. **d**, **d'** Effects of miR-375 and HGF treatment on the protein level of PDK1 in MSCs. Cells infected with Ad-375 or Ad for 48 h were incubated with L-DMEM or L-DMEM containing 50 ng/ml HGF for different times after 30 min starvation. Total cell lysates were resolved in SDS-PAGE, and immunoprecipitated with antibody against PDK1. β-actin served as a loading control. The level of PDK1 was measured by densitometry of immunoreactive bands using ImageJ software. Shown are representative results of three independent experiments, data presented are mean ± SEM. *$P < 0.05$ vs. Ad. **e** HGF decreases the expression of miR-375 in MSCs infected with Ad-375. Expression of miR-375 was normalized with U6 snRNA and expressed as a percentage of Ad-infected cells without HGF treatment. Data presented are mean ± SEM from three independent experiments. *$P < 0.05$ vs Ad-375 without HGF

and paxillin, especially at Tyr397 of FAK (Y397-FAK) and Tyr118 of paxillin (Y118-paxillin) (Deramaudt et al. 2014; Hamadi et al. 2005; Zaidel-Bar et al. 2007). We subsequently investigated whether they are involved in the miR-375-suppressed motility of MSCs. The results showed that phosphorylation levels of Y397-FAK (Y397-P) and Y118-paxillin (Y118-P) were significantly lowered in MSCs overexpressing miR-375 (Fig. 7a–b'). HGF treatment for 15–30 min enhanced the level of Y397-P and Y118-P in both control and miR-375-overexpressing cells (Fig. 7c–c''); however, Y397-P and Y118-P in miR-375-overexpressing cells remained at much lower levels than in control cells upon HGF treatment (Fig. 7c–c''), reminiscent of the downregulation of Y397-P and Y118-P by miR-375 (Fig. 7a–b'). These results demonstrate that miR-375 inhibits the phosphorylation of Y397-FAK and Y118-paxillin, which might contribute to the changed lengths and decreased peripheral distribution of FAs in miR-375-overexpressing cells compared with control cells, thereby leading to the impaired migration.

Discussion

Cell migration is an essential process that occurs both physiologically and pathologically. Accumulating evidence demonstrates that miRNAs are important regulators of cell migration (Huang and He 2010). Dysregulation of miRNA abundance is closely linked with migration-related diseases, for example, tumor and cancer invasiveness and metastasis (Baranwal and Alahari 2010). However, miRNA's effects on the migration of MSCs remain largely unknown. Using microarrays, we found 26 differentially expressed miRNAs in MSCs treated with HGF (Zhu et al. 2016). Two upregulated miRNAs, miR-26b and miR-221, were found to promote MSC migration by targeting PTEN and activating Akt and FAK signaling pathways (Zhu et al. 2016). In this study, we report that one HGF-downregulated miRNA, miR-375, is also involved in regulating HGF-elicited migration of MSCs in a way different from miR-26b and miR-221.

Using a Boyden chamber, we verified that overexpression of miR-375, achieved by infecting MSCs with Ad-375, a recombinant adenovirus containing the miR-375 precursor sequence, significantly impaired HGF-elicited migration (Fig. 2b, b'). Time-lapse video microscopy revealed that miR-375 had little effect on the migration velocity and persistency when HGF were not in the assay system (Fig. 3c, c'), but significantly attenuated the migration velocity when 50 ng/ml HGF was in the outer well of the Dunn chamber (Fig. 3d). These results suggest that miR-375 participates in the regulation of HGF-elicited migration of MSCs.

Growth factors, such as HGF and VEGF, stimulate cell migration by activating numerous elements of signaling transduction (Forte et al. 2006; Higuchi et al. 2013; Ponte et al. 2007; Xu et al. 2014). Our previous data reveal that PI3K/Akt and MAPK signalings are involved in the regulation of MSC migration toward HGF (Zheng et al. 2013). We found that overexpression of miR-375 had little effect on the phosphorylation of ERK1/2, p38MAPK, and SAPK/JNK, but strongly decreased the phosphorylation of Akt at both T308 and S473 (Fig. 4). Thus, it seems unlikely that MAPK signaling mediates the influence of miR-375 on MSC migration. Consistently, there is evidence showing that miR-375 suppresses pancreatic carcinoma cell growth through the Akt rather than the MAPK signaling pathway (Zhou et al. 2014).

Maximal activation of Akt requires its phosphorylation at both T308 and S473, which is catalyzed by PDK1 (Alessi et al. 1997), and mTORC2 (Sarbassov et al. 2005). Phosphorylation defect of either residue will decrease the activity of Akt (Alessi et al. 1997; Mora et al. 2003, 2005; Sarbassov et al. 2005; Williams et al. 2000). PDK1 has been demonstrated to be a direct target of miR-375 in rat pancreatic β-cells (El Ouaamari et al. 2008). Consistently, we found that overexpression of miR-375 significantly downregulated the expression of PDK1 (Fig. 5c–d'), thereby leading to decreased phosphorylation of Akt (Fig. 4). Exposure to HGF significantly decreased the level of miR-375 in MSCs both endogenously (Fig. 1) and exogenously (Fig. 5e), but increased the protein level of PDK1 (Fig. 5c–d') and, slightly, the phosphorylation level of Akt at T308 (Fig. 4c, c''). However, the overall levels of PDK1 (Fig. 5c–d') and Akt phosphorylation at T308 (Fig. 4b, b', c, c'') in miR-375-overexpressing cells remained lower than those in control cells, suggesting that miR-375 inhibits the HGF-induced Akt activation by downregulating the expression of PDK1. There is evidence showing that a deficiency of PDK1 results in a complete depletion of Akt phosphorylation at T308 and an increase of phosphorylation at S473 in embryonic stem cells, cardiac muscle and liver cells (Mora et al. 2003, 2005; Williams et al. 2000). However, we observed that downregulation of Akt phosphorylation at T308 by miR-375-depleted PDK1 expression was accompanied by decreased Akt phosphorylation at S473 in MSCs (Figs. 4, 5). This discrepancy might be attributable to other targets of miR-375 that regulate the phosphorylation of Akt at S473. Indeed, consistent with our results, recent studies have shown that miR-375 inhibits Akt phosphorylation at S473 in MSCs by directly targeting DEPTOR, an endogenous mTOR inhibitor (Chen et al. 2017; Peterson et al. 2009).

In addition to protein kinase PDK1 and mTORC2, the phosphorylation of Akt at T308 and S473 is negatively regulated by protein phosphatase 2A (PP2A) and PH domain leucine-rich repeat protein phosphatase 1 (PHLPP1), respectively (Gao et al. 2005; Millward et al. 1999). Using TargetScan and miRDB, MiR-375 is predicted to target the regulatory subunit B alpha of PP2A, which may decrease the activity of PP2A and thereby increase the phosphorylation of Akt at T308. MiR-375 has also been shown to target PHLPP1,

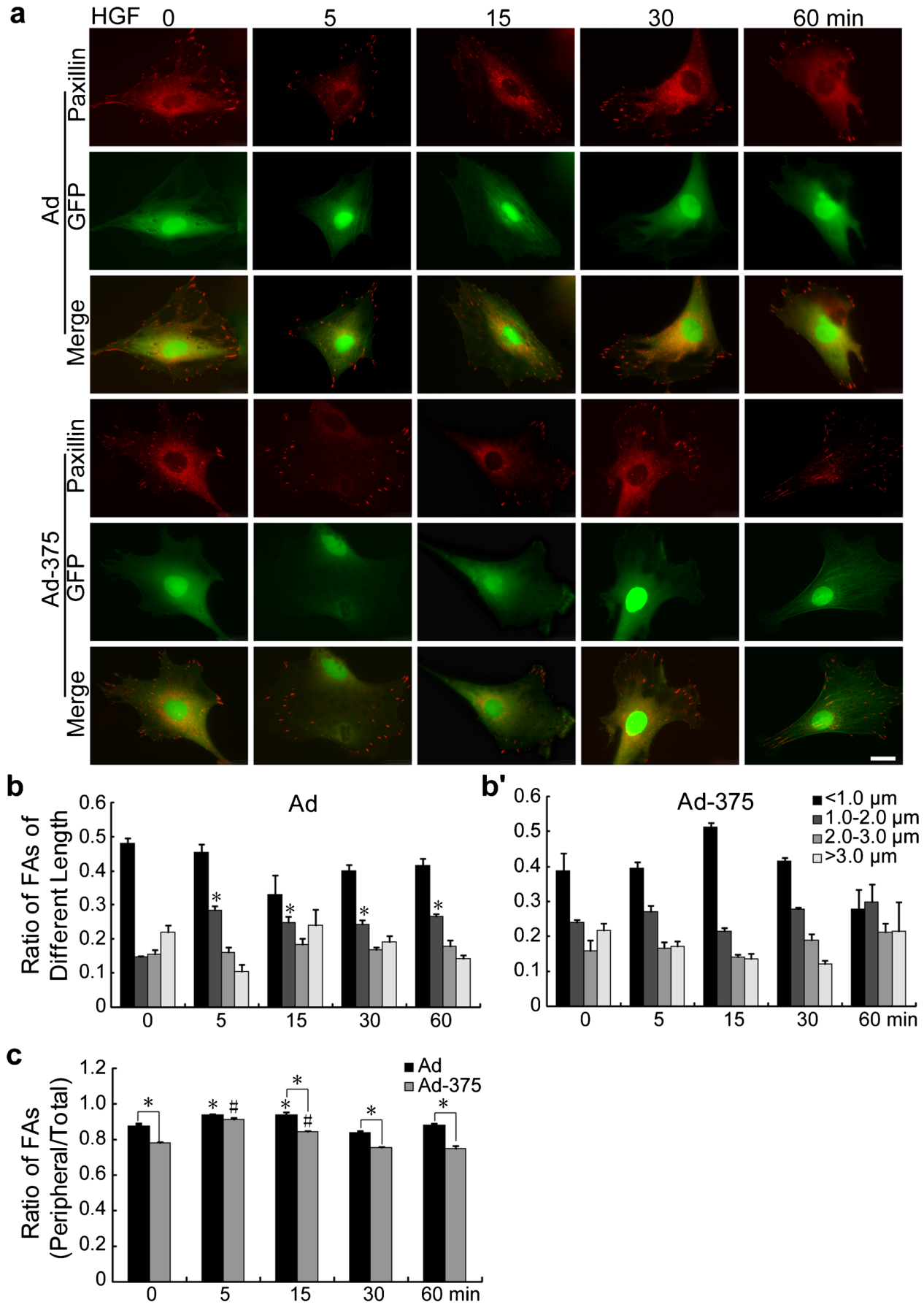
a
HGF 0
5
15
30
60 min
Ad
Paxillin
GFP
Merge
Ad-375
Paxillin
GFP
Merge
b
Ad
Ratio of FAs of Different Length
0
0.1
0.2
0.3
0.4
0.5
0.6
0
5
15
30
60
b'
Ad-375
<1.0 μm
1.0-2.0 μm
2.0-3.0 μm
>3.0 μm
0
5
15
30
60 min
c
Ratio of FAs (Peripheral/Total)
Ad
Ad-375
0
0.2
0.4
0.6
0.8
1.0
1.2
0
5
15
30
60 min

◀ **Fig. 6** MiR-375 influences the length and distribution of focal adhesions (FAs) upon HGF treatment. **a** Representative images of FAs by paxillin immunostaining in MSCs infected with Ad or Ad-375 and treated with 50 ng/ml HGF for indicated times. *Scale bar* 25 μm. **b**, **b'** Ratio of FAs at different length in Ad- or Ad-375-infected MSCs. **c** Ratio of FAs at cell periphery to total number of FAs in Ad- or Ad-375-infected MSCs. Values are mean ± SEM from three independent experiments. **P* < 0.05 vs. Ad without HGF. #*P* < 0.05 vs. Ad-375 without HGF

a negative regulator of Akt phosphorylation at S473 in prostate carcinomas (Hart et al. 2014). However, our results showed that overexpression of miR-375 leads to the decrease of Akt phosphorylation at T308 and S473. Altogether, it seems unlikely that miR-375 acts through phosphatases PP2A and PHLPP1 to decrease the phosphorylation of Akt at T308 and S473, thereby regulating the migration of MSCs.

PDK1 has been recognized as a key regulator of cell migration triggered by growth factors and other extracellular signals (Gagliardi et al. 2015), and Akt is about the most important transducer that is required for cell migration downstream of PDK1. The results presented here, combined with

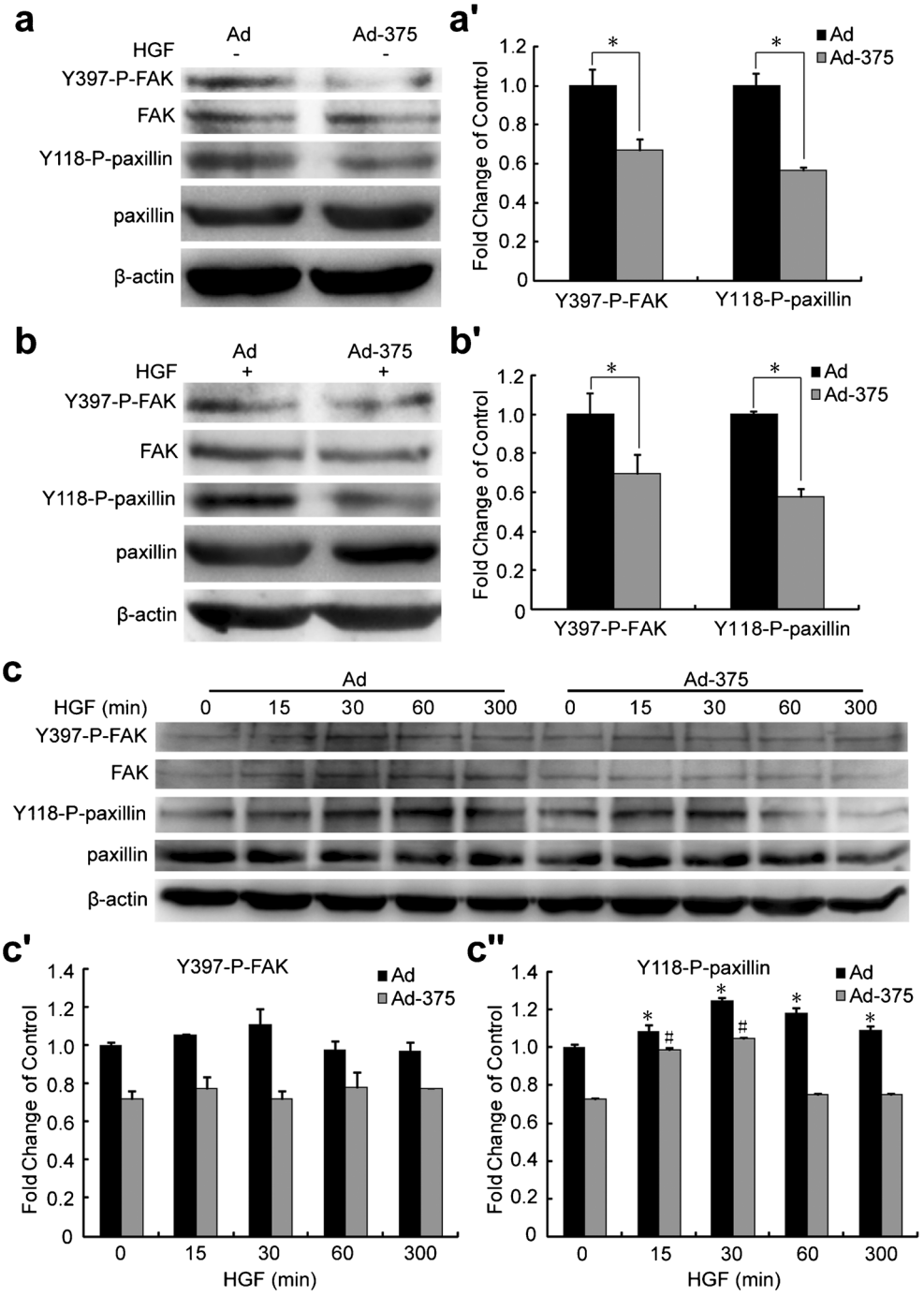

Fig. 7 MiR-375 suppresses the activity of FAK and paxillin. **a**, **a'** Tyrosine phosphorylation of FAK at 397 (Y397-P) and paxillin at 118 (Y118-P) in MSCs infected with Ad-375 or Ad before HGF treatment. **b**, **b'** Tyrosine phosphorylation of Y397-FAK and Y118-paxillin in MSCs infected with Ad-375 or Ad after HGF stimulation for 30 min. **c**, **c'**, **c''** Tyrosine phosphorylation of Y397-FAK and Y118-paxillin in MSCs infected with Ad-375 or Ad upon HGF treatment for indicated times. Adenovirus infection and HGF treatment of MSCs were the same as described in Fig. 4. Shown are representative results of three independent experiments, data presented are mean ± SEM. **P* < 0.05 vs. Ad without HGF. #*P* < 0.05 vs. Ad-375 without HGF

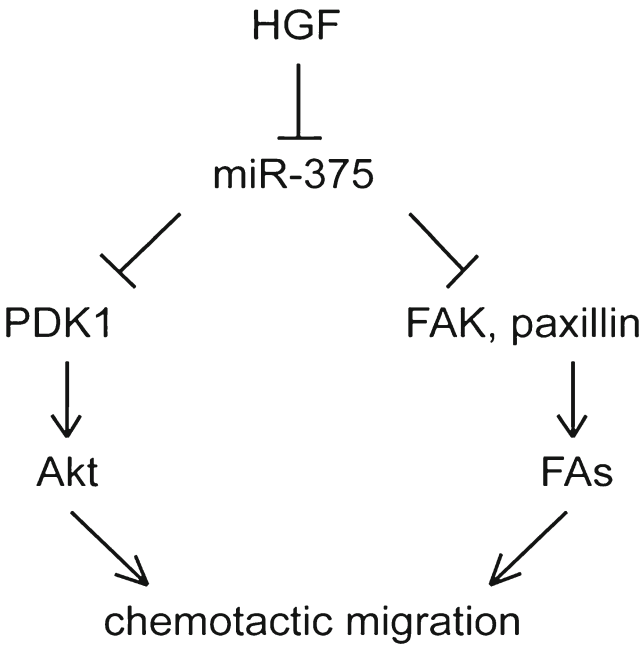

Fig. 8 The proposed signaling molecules and the role of miR-375 in modulating the chemotactic migration of MSCs

our previous findings that another two HGF-upregulated miRNAs, miR-26b and miR-221, promote MSC migration by targeting PTEN and activating Akt (Zhu et al. 2016), allow us to conclude that downregulation of miR-375 and upregulation of miR-26b and miR-221 in response to HGF stimulation coordinate the activation of the Akt signaling pathway and promote the migration of MSCs. However, the detailed molecular mechanism downstream of Akt, which directly mediates the effects of miR-375, miR-26b and miR-221 on MSC migration, requires further elucidation.

Coordinate assembly, disassembly and maturation of FAs are required for persistent cell migration. Nascent adhesions, initially formed and localized immediately behind the leading edge, are small and usually undergo rapid turnover, unless they mature to form typical focal adhesions of approximately 1 μm in diameter in response to tensile stress (Parsons et al. 2010; Zaidel-Bar et al. 2003). Most of these FAs disassemble upon retraction of the lamella and the remaining mature into elongated, larger and more stable FAs, usually 3–10 μm long and localized further within the cell (Parsons et al. 2010; Zaidel-Bar et al. 2003). Small FAs of approximately 1 μm in diameter are more dynamic and peripherally distributed and mediate traction forces required for cell migration, whereas larger FAs, typically 3–10 μm long and centrally distributed, mediate cell spreading (Fogh et al. 2014; Parsons et al. 2010). In this study. we found that overexpression of miR-375 interfered the HGF-induced formation of small FAs (1–2 μm long), and decreased the number of FAs localized at the periphery (Fig. 6b, b', c). These results suggest that miR-375 might affect the HGF-induced formation of peripheral small FAs, thereby leading to the inhibition of cell migration.

Tyrosine phosphorylation of FAK and paxillin has been proved to regulate FA dynamics (Hamadi et al. 2005; Zaidel-Bar et al. 2007). Reduced tyrosine phosphorylation of FAK leads to larger and more stable FAs and slower FA turnover (Deramaudt et al. 2011; Ilic et al. 1995; Volberg et al. 2001; Webb et al. 2004). Paxillin phosphorylation at Y118 promotes cell migration, enhancing the formation and turnover of adhesions (Zaidel-Bar et al. 2007). In the present study, miR-375 suppressed the phosphorylation of Y397-FAK and Y118-paxillin (Fig. 7), which might contribute to the influence of miR-375 on FAs.

FAK has been typically considered upstream of Akt through direct binding of PI3K and PTEN (Tamura et al. 1999; Xia et al. 2004). Recent studies have proved that Akt facilitates tyrosine phosphorylation of FAK by directly binding and phosphorylating three serine sites of FAK (Tureckova et al. 2009; Wang and Basson 2011). These results suggest that mutual regulation or interaction may exist between Akt and FAK. Their relationship in mediating the miR-375-inhibited migration of MSCs requires further investigation.

In conclusion (Fig. 8), we demonstrate that miR-375 inhibits HGF-elicited migration of MSCs by downregulating PDK1 and its downstream Akt signaling. Moreover, miR-375 prevents the peripheral distribution of FAs and decreases the phosphorylation of Y397-FAK and Y118-paxillin upon HGF stimulation, which might also contribute to the inhibition of cell migration by miR-375. These results provide novel insights into the mechanism of cell migration elicited by HGF, which may benefit the cell-based therapy in the future by manipulating the level of miR-375 and improving the homing capability of transplanted MSCs.

Acknowledgements This work was supported by the National Natural Science Foundation of China (Grant no. 31371407, 30870642) and the Priority Academic Program Development of Jiangsu Higher Education Institutions.

Author contributions LH and HZ designed the study, conducted all searches, appraised all potential studies and wrote and revised the draft manuscript and subsequent manuscripts. XW conceived and designed the study, assisted with searches, appraised relevant studies and assisted with drafting and revising the manuscript. NK assisted with searches and appraised relevant studies. JX, ND and XX assisted with drafting and revising the manuscript. All authors read and approved the final manuscript.

Compliance with ethical standards

Conflict of interest The authors declare no conflict of interest.

References

Abdallah BM, Kassem M (2008) Human mesenchymal stem cells: from basic biology to clinical applications. Gene Ther 15:109–116

Alessi DR, James SR, Downes CP, Holmes AB, Gaffney PR, Reese CB, Cohen P (1997) Characterization of a 3-phosphoinositide-dependent

protein kinase which phosphorylates and activates protein kinase Balpha. Curr Biol 7:261–269
Baranwal S, Alahari SK (2010) miRNA control of tumor cell invasion and metastasis. Int J Cancer 126:1283–1290
Bianco P, Riminucci M, Gronthos S, Robey PG (2001) Bone marrow stromal stem cells: nature, biology, and potential applications. Stem Cells 19:180–192
Chamberlain G, Fox J, Ashton B, Middleton J (2007) Concise review: mesenchymal stem cells: their phenotype, differentiation capacity, immunological features, and potential for homing. Stem Cells 25: 2739–2749
Chen S, Zheng YF, Zhang S, Jia LF, Zhou YS (2017) Promotion effects of miR-375 on the Osteogenic differentiation of human adipose-derived Mesenchymal stem cells. Stem Cell Rep 8:773–786
Cho KJ, Trzaska KA, Greco SJ, Mcardle J, Wang FS, Ye JH, Rameshwar P (2005) Neurons derived from human mesenchymal stem cells show synaptic transmission and can be induced to produce the neurotransmitter substance P by interleukin-1 alpha. Stem Cells 23: 383–391
Deramaudt TB, Dujardin D, Hamadi A, Noulet F, Kolli K, De Mey J, Takeda K, Ronde P (2011) FAK phosphorylation at Tyr-925 regulates cross-talk between focal adhesion turnover and cell protrusion. Mol Biol Cell 22:964–975
Deramaudt TB, Dujardin D, Noulet F, Martin S, Vauchelles R, Takeda K, Ronde P (2014) Altering FAK-paxillin interactions reduces adhesion, migration and invasion processes. PLoS ONE 9:e92059
Dezawa M, Kanno H, Hoshino M, Cho H, Matsumoto N, Itokazu Y, Tajima N, Yamada H, Sawada H, Ishikawa H, Mimura T, Kitada M, Suzuki Y, Ide C (2004) Specific induction of neuronal cells from bone marrow stromal cells and application for autologous transplantation. J Clin Invest 113:1701–1710
El Ouaamari A, Baroukh N, Martens GA, Lebrun P, Pipeleers D, Van Obberghen E (2008) miR-375 targets 3′-phosphoinositide-dependent protein kinase-1 and regulates glucose-induced biological responses in pancreatic beta-cells. Diabetes 57:2708–2717
El-Hossary N, Hassanein H, El-Ghareeb AW, Issa H (2016) Intravenous vs intraperitoneal transplantation of umbilical cord mesenchymal stem cells from Wharton's jelly in the treatment of streptozotocin-induced diabetic rats. Diabetes Res Clin Pract 121:102–111
English K, French A, Wood KJ (2010) Mesenchymal stromal cells: facilitators of successful transplantation? Cell Stem Cell 7:431–442
Fogh BS, Multhaupt HA, Couchman JR (2014) Protein kinase C, focal adhesions and the regulation of cell migration. J Histochem Cytochem 62:172–184
Forte G, Minieri M, Cossa P, Antenucci D, Sala M, Gnocchi V, Fiaccavento R, Carotenuto F, De Vito P, Baldini PM, Prat M, Di Nardo P (2006) Hepatocyte growth factor effects on mesenchymal stem cells: proliferation, migration, and differentiation. Stem Cells 24:23–33
Gagliardi PA, Di Blasio L, Primo L (2015) PDK1: A signaling hub for cell migration and tumor invasion. Biochim Biophys Acta 1856: 178–188
Gao T, Furnari F, Newton AC (2005) PHLPP: a phosphatase that directly dephosphorylates Akt, promotes apoptosis, and suppresses tumor growth. Mol Cell 18:13–24
Garofalo M, Di Leva G, Romano G, Nuovo G, Suh SS, Ngankeu A, Taccioli C, Pichiorri F, Alder H, Secchiero P, Gasparini P, Gonelli A, Costinean S, Acunzo M, Condorelli G, Croce CM (2009) miR-221&222 regulate TRAIL resistance and enhance tumorigenicity through PTEN and TIMP3 downregulation. Cancer Cell 16:498–509
Hamadi A, Bouali M, Dontenwill M, Stoeckel H, Takeda K, Ronde P (2005) Regulation of focal adhesion dynamics and disassembly by phosphorylation of FAK at tyrosine 397. J Cell Sci 118:4415–4425
Hart M, Nolte E, Wach S, Szczyrba J, Taubert H, Rau TT, Hartmann A, Grasser FA, Wullich B (2014) Comparative microRNA profiling of prostate carcinomas with increasing tumor stage by deep sequencing. Mol Cancer Res 12:250–263
Higuchi M, Kihara R, Okazaki T, Aoki I, Suetsugu S, Gotoh Y (2013) Akt1 Promotes focal adhesion disassembly and cell motility through phosphorylation of FAK in growth factor-stimulated cells. J Cell Sci 126:745–755
Huang S, He X (2010) microRNAs: tiny RNA molecules, huge driving forces to move the cell. Protein Cell 1:916–926
Ilic D, Furuta Y, Kanazawa S, Takeda N, Sobue K, Nakatsuji N, Nomura S, Fujimoto J, Okada M, Yamamoto T (1995) Reduced cell motility and enhanced focal adhesion contact formation in cells from FAK-deficient mice. Nature 377:539–544
Im HI, Kenny PJ (2012) MicroRNAs in neuronal function and dysfunction. Trends Neurosci 35:325–334
Kinoshita T, Hanazawa T, Nohata N, Okamoto Y, Seki N (2012) The functional significance of microRNA-375 in human squamous cell carcinoma: aberrant expression and effects on cancer pathways. J Hum Genet 57:556–563
Kong KL, Kwong DL, Chan TH, Law SY, Chen L, Li Y, Qin YR, Guan XY (2012) MicroRNA-375 inhibits tumour growth and metastasis in oesophageal squamous cell carcinoma through repressing insulin-like growth factor 1 receptor. Gut 61:33–42
Kwon JS, Kim SW, Kwon DY, Park SH, Son AR, Kim JH, Kim MS (2014) In vivo osteogenic differentiation of human turbinate mesenchymal stem cells in an injectable in situ-forming hydrogel. Biomaterials 35:5337–5346
Li N, Fu H, Tie Y, Hu Z, Kong W, Wu Y, Zheng X (2009) miR-34a inhibits migration and invasion by down-regulation of c-met expression in human hepatocellular carcinoma cells. Cancer Lett 275:44–53
Livak KJ, Schmittgen TD (2001) Analysis of relative gene expression data using real-time quantitative PCR and the 2(−Delta Delta C(T)) method. Methods 25:402–408
Luk JM, Wang PP, Lee CK, Wang JH, Fan ST (2005) Hepatic potential of bone marrow stromal cells: development of in vitro co-culture and intra-portal transplantation models. J Immunol Methods 305:39–47
Marconi S, Castiglione G, Turano E, Bissolotti G, Angiari S, Farinazzo A, Constantin G, Bedogni G, Bedogni A, Bonetti B (2012) Human adipose-derived mesenchymal stem cells systemically injected promote peripheral nerve regeneration in the mouse model of sciatic crush. Tissue Eng Part A 18:1264–1272
Meng F, Henson R, Wehbe-Janek H, Ghoshal K, Jacob ST, Patel T (2007) MicroRNA-21 regulates expression of the PTEN tumor suppressor gene in human hepatocellular cancer. Gastroenterology 133:647–658
Millward TA, Zolnierowicz S, Hemmings BA (1999) Regulation of protein kinase cascades by protein phosphatase 2A. Trends Biochem Sci 24:186–191
Mora A, Davies AM, Bertrand L, Sharif I, Budas GR, Jovanovic S, Mouton V, Kahn CR, Lucocq JM, Gray GA, Jovanovic A, Alessi DR (2003) Deficiency of PDK1 in cardiac muscle results in heart failure and increased sensitivity to hypoxia. EMBO J 22:4666–4676
Mora A, Lipina C, Tronche F, Sutherland C, Alessi DR (2005) Deficiency of PDK1 in liver results in glucose intolerance, impairment of insulin-regulated gene expression and liver failure. Biochem J 385: 639–648
Murphy MB, Moncivais K, Caplan AI (2013) Mesenchymal stem cells: environmentally responsive therapeutics for regenerative medicine. Exp Mol Med 45:e54
Parr AM, Tator CH, Keating A (2007) Bone marrow-derived mesenchymal stromal cells for the repair of central nervous system injury. Bone Marrow Transplant 40:609–619
Parsons JT, Horwitz AR, Schwartz MA (2010) Cell adhesion: integrating cytoskeletal dynamics and cellular tension. Nat Rev Mol Cell Biol 11:633–643

Peterson TR, Laplante M, Thoreen CC, Sancak Y, Kang SA, Kuehl WM, Gray NS, Sabatini DM (2009) DEPTOR is an mTOR inhibitor frequently Overexpressed in multiple myeloma cells and required for their survival. Cell 137:873–886

Pittenger MF, Mackay AM, Beck SC, Jaiswal RK, Douglas R, Mosca JD, Moorman MA, Simonetti DW, Craig S, Marshak DR (1999) Multilineage potential of adult human mesenchymal stem cells. Science 284:143–147

Ponte AL, Marais E, Gallay N, Langonne A, Delorme B, Herault O, Charbord P, Domenech J (2007) The in vitro migration capacity of human bone marrow mesenchymal stem cells: comparison of chemokine and growth factor chemotactic activities. Stem Cells 25: 1737–1745

Ryu CH, Park SA, Kim SM, Lim JY, Jeong CH, Jun JA, Oh JH, Park SH, Oh WI, Jeun SS (2010) Migration of human umbilical cord blood mesenchymal stem cells mediated by stromal cell-derived factor-1/CXCR4 axis via Akt, ERK, and p38 signal transduction pathways. Biochem Biophys Res Commun 398:105–110

Sarbassov DD, Guertin DA, Ali SM, Sabatini DM (2005) Phosphorylation and regulation of Akt/PKB by the rictor-mTOR complex. Science 307:1098–1101

Schenk S, Mal N, Finan A, Zhang M, Kiedrowski M, Popovic Z, Mccarthy PM, Penn MS (2007) Monocyte chemotactic protein-3 is a myocardial mesenchymal stem cell homing factor. Stem Cells 25:245–251

Song J, Kim D, Chun CH, Jin EJ (2013) MicroRNA-375, a new regulator of cadherin-7, suppresses the migration of chondrogenic progenitors. Cell Signal 25:698–706

Sordi V, Malosio ML, Marchesi F, Mercalli A, Melzi R, Giordano T, Belmonte N, Ferrari G, Leone BE, Bertuzzi F, Zerbini G, Allavena P, Bonifacio E, Piemonti L (2005) Bone marrow mesenchymal stem cells express a restricted set of functionally active chemokine receptors capable of promoting migration to pancreatic islets. Blood 106: 419–427

Stock P, Bruckner S, Ebensing S, Hempel M, Dollinger MM, Christ B (2010) The generation of hepatocytes from mesenchymal stem cells and engraftment into murine liver. Nat Protoc 5:617–627

Tamura M, Gu J, Danen EH, Takino T, Miyamoto S, Yamada KM (1999) PTEN interactions with focal adhesion kinase and suppression of the extracellular matrix-dependent phosphatidylinositol 3-kinase/Akt cell survival pathway. J Biol Chem 274:20693–20703

Tome M, Lopez-Romero P, Albo C, Sepulveda JC, Fernandez-Gutierrez B, Dopazo A, Bernad A, Gonzalez MA (2011) miR-335 orchestrates cell proliferation, migration and differentiation in human mesenchymal stem cells. Cell Death Differ 18:985–995

Tureckova J, Vojtechova M, Krausova M, Sloncova E, Korinek V (2009) Focal adhesion kinase functions as an akt downstream target in migration of colorectal cancer cells. Transl Oncol 2:281–290

Volberg T, Romer L, Zamir E, Geiger B (2001) pp60(C-src) and related tyrosine kinases: a role in the assembly and reorganization of matrix adhesions. J Cell Sci 114:2279–2289

Wang H, Wang X, Qu J, Yue Q, Hu Y, Zhang H (2015) VEGF enhances the migration of MSCs in neural differentiation by regulating focal adhesion turnover. J Cell Physiol 230:2728–2742

Wang M, Liang C, Hu H, Zhou L, Xu B, Wang X, Han Y, Nie Y, Jia S, Liang J, Wu K (2016) Intraperitoneal injection (IP), intravenous injection (IV) or anal injection (AI)? Best way for mesenchymal stem cells transplantation for colitis. Sci Rep 6:30696

Wang S, Basson MD (2011) Akt directly regulates focal adhesion kinase through association and serine phosphorylation: implication for pressure-induced colon cancer metastasis. Am J Physiol Cell Physiol 300:C657–C670

Webb DJ, Donais K, Whitmore LA, Thomas SM, Turner CE, Parsons JT, Horwitz AF (2004) FAK-Src signalling through paxillin, ERK and MLCK regulates adhesion disassembly. Nat Cell Biol 6:154–161

Williams MR, Arthur JS, Balendran A, Van Der Kaay J, Poli V, Cohen P, Alessi DR (2000) The role of 3-phosphoinositide-dependent protein kinase 1 in activating AGC kinases defined in embryonic stem cells. Curr Biol 10:439–448

Xia H, Nho RS, Kahm J, Kleidon J, Henke CA (2004) Focal adhesion kinase is upstream of phosphatidylinositol 3-kinase/Akt in regulating fibroblast survival in response to contraction of type I collagen matrices via a beta 1 integrin viability signaling pathway. J Biol Chem 279:33024–33034

Xu X, Xie G, Hu Y, Li X, Huang P, Zhang H (2014) Neural differentiation of mesenchymal stem cells influences their chemotactic responses to stromal cell-derived factor-1alpha. Cell Mol Neurobiol 34:1047–1058

Yan D, Dong Xda E, Chen X, Wang L, Lu C, Wang J, Qu J, Tu L (2009) MicroRNA-1/206 targets c-met and inhibits rhabdomyosarcoma development. J Biol Chem 284:29596–29604

Zaidel-Bar R, Ballestrem C, Kam Z, Geiger B (2003) Early molecular events in the assembly of matrix adhesions at the leading edge of migrating cells. J Cell Sci 116:4605–4613

Zaidel-Bar R, Milo R, Kam Z, Geiger B (2007) A paxillin tyrosine phosphorylation switch regulates the assembly and form of cell-matrix adhesions. J Cell Sci 120:137–148

Zhang F, Jing S, Ren T, Lin J (2013) MicroRNA-10b promotes the migration of mouse bone marrow-derived mesenchymal stem cells and downregulates the expression of E-cadherin. Mol Med Rep 8:1084–1088

Zheng B, Wang C, He L, Xu X, Qu J, Hu J, Zhang H (2013) Neural differentiation of mesenchymal stem cells influences chemotactic responses to HGF. J Cell Physiol 228:149–162

Zhou J, Song S, He S, Zhu X, Zhang Y, Yi B, Zhang B, Qin G, Li D (2014) MicroRNA-375 targets PDK1 in pancreatic carcinoma and suppresses cell growth through the Akt signaling pathway. Int J Mol Med 33:950–956

Zhu A, Kang N, He L, Li X, Xu X, Zhang H (2016) MiR-221 and miR-26b regulate Chemotactic migration of MSCs toward HGF through activation of Akt and FAK. J Cell Biochem 117:1370–1383